Focal adhesion kinase-Tyr^{407} and -Tyr^{397} exhibit antagonistic effects on blood–testis barrier dynamics in the rat

Pearl P. Y. Lie[a], Dolores D. Mruk[a], Ka Wai Mok[a], Linlin Su[a], Will M. Lee[b], and C. Yan Cheng[a,1]

[a]The Mary M. Wohlford Laboratory for Male Contraceptive Research, Center for Biomedical Research, Population Council, New York, NY 10065; and [b]School of Biological Sciences, University of Hong Kong, Hong Kong, China

Focal adhesion kinase (FAK), a nonreceptor protein tyrosine kinase, displays phosphorylation-dependent localization in the seminiferous epithelium of adult rat testes. FAK is an integrated component of the blood–testis barrier (BTB) involved in regulating Sertoli cell adhesion via its effects on the occludin–zonula occludens-1 complex. Herein, we report that p-FAK-Tyr^{407} and p-FAK-Tyr^{397} display restricted spatiotemporal and almost mutually exclusive localization in the epithelium, affecting BTB dynamics antagonistically, with the former promoting and the latter disrupting the Sertoli cell tight junction–permeability barrier function. Using primary cultured Sertoli cells as an in vitro model that mimics the BTB in vivo both functionally and ultrastructurally, effects of FAK phosphorylation on BTB function were studied by expressing nonphosphorylatable and phosphomimetic mutants, with tyrosine replaced by phenylalanine (F) and glutamate (E), respectively. Compared with WT FAK, Y407E and Y397F mutations each promoted barrier function, and the promoting effect of the Y407E mutant was abolished in the Y397E-Y407E double mutant, demonstrating antagonism between Tyr^{407} and Tyr^{397}. Furthermore, Y407E mutation induced the recruitment of actin-related protein 3 to the Sertoli cell-cell interface, where it became more tightly associated with neuronal Wiskott–Aldrich syndrome protein, promoting actin-related protein 2/3 complex activity. Conversely, Y407F mutation reduced the rate of actin polymerization at the Sertoli cell BTB. In summary, FAK-Tyr^{407} phosphorylation promotes BTB integrity by strengthening the actin filament-based cytoskeleton. FAK serves as a bifunctional molecular "switch" to direct the cyclical disassembly and reassembly of the BTB during the epithelial cycle of spermatogenesis, depending on its phosphorylation status, to facilitate the transit of preleptotene spermatocytes across the BTB.

actin filament network | ectoplasmic specialization

In the seminiferous epithelium, the blood–testis barrier (BTB) created by coexisting tight junction (TJ) and basal ectoplasmic specialization [basal ES, a testis-specific adherens junction (AJ)] between Sertoli cells near the basement membrane is one of the tightest blood–tissue barriers in the mammalian body (1). This is attributable to the tightly packed actin filament bundles sandwiched between cisternae of endoplasmic reticulum and the apposing Sertoli cell plasma membrane at the basal ES, the hallmark ultrastructure of the BTB (1). However, the BTB undergoes cyclical restructuring to allow the transit of preleptotene spermatocytes from the basal to the adluminal compartment in the rat (1, 2), implying that these filament bundles undergo extensive reorganization. Previous studies have shown that focal adhesion kinase (FAK) is predominantly localized in the seminiferous epithelium near the basement membrane at the site of the BTB (3), whereas its phosphorylated form, p-FAK-Tyr^{397}, is almost exclusively restricted to the apical ES (3, 4) [a filamentous (F)-actin–rich testis-specific AJ, analogous to the basal ES structurally but limited to the Sertoli cell-spermatid interface, which also undergoes cyclical remodeling to facilitate spermatid movement across the epithelium during spermiogenesis (2, 5)].

Recent studies have shown that FAK is a regulatory protein that modulates TJ integrity at the BTB via its effects on the phosphorylation status of the adhesion protein complexes, such as the occludin–zonula occludens (ZO)-1 complex (6). Its effects on the F-actin network, if any, remain unknown.

FAK is known to regulate focal adhesion complexes, which are anchoring junctions at the cell-matrix interface in multiple epithelia and migrating cells. When activated by integrin clustering or ligand binding of growth factor (e.g., TGF-β) receptors, FAK plays a central role in transducing signals to the actin cytoskeleton to elicit F-actin remodeling (e.g., formation of lamellipodia and stress fibers) during cell adhesion and migration (1, 7). For instance, FAK is known to interact with a number of guanine-nucleotide exchange factors and GTPase-activating proteins, which, in turn, regulate the activation status of Rho family GTPases, such as Rac and Rho (8, 9), and actin cytoskeleton (10). FAK has recently been shown to influence actin-related protein (Arp) 2/3 complex-mediated actin nucleation, modulating actin cytoskeleton, through at least two mechanisms. These include blockade of neuronal Wiskott–Aldrich syndrome protein (N-WASP), an Arp2/3 activator (11), from entering the nucleus following FAK-mediated phosphorylation (12), as well as the direct interaction of FAK 4.1/ezrin/radixin/moesin domain with Arp3, which enhances Arp2/3 activity (13). In short, FAK harnesses multiple levels of control over actin polymerization. Interestingly, FAK/Arp3 interaction is negatively regulated by the phosphorylation of FAK-Tyr^{397}, which is the major autophosphorylation site induced by integrin signaling (13). However, additional regulation by yet to be defined phosphorylation events is clearly at play, because Arp3 binding to FAK Y397F (nonphosphorylatable mutant) was further enhanced in suspended cells vs. adhered cells (13). In an effort to understand the possible involvement of other FAK phosphorylation sites in actin dynamics better, we found that p-FAK-Tyr^{407} was recruited to actin-rich ultrastructures: the basal ES and the apical ES. Herein, we report that FAK-Tyr^{407} phosphorylation exhibits antagonism with Tyr^{397} in regulating Sertoli cell TJ integrity and that FAK-Tyr^{407} phosphorylation is key to the regulation of N-WASP–Arp2/3 complex activity at the BTB.

Results

FAK Phosphorylation at Tyr^{407} and Tyr^{397} Is Spatiotemporally Restricted in the Seminiferous Epithelium with Distinctive Localization Patterns.
FAK and two of its phosphorylated forms, p-FAK-Tyr^{407} and p-FAK-Tyr^{397}, were detected in lysates of adult rat testes, Sertoli

cells, and germ cells (Fig. 1A) using phosphospecific anti-FAK antibodies (Table S1). Expression of the two phosphorylated forms was highest in Sertoli cells (Fig. 1B). Because the localization of p-FAK-Tyr^{407} in the testis has not been reported, immunofluorescence staining was performed to study its expression using a specific antibody (Fig. 1 C–E and Table S1). In all stages of the epithelial cycle, p-FAK-Tyr^{407} was expressed at the Sertoli cell-cell interface at the BTB (Fig. 1D), where it colocalized with total FAK, F-actin, Arp3, and the TJ protein ZO-1 (Fig. S1). The p-FAK-Tyr^{407} was also found at the adhesion sites between Sertoli cells and elongating/elongated spermatids known as apical ES. Most notably, p-FAK-Tyr^{407} was intensely localized to the concave side of elongated spermatid heads in stage VII to early stage VIII tubules (Fig. 1E), corresponding to an ultrastructure formerly designated the apical tubulobulbar complex (apical TBC), which is reminiscent of aggregated endocytic vesicles of junction complex proteins (e.g., cadherins, integrins) derived from the degenerating apical ES during spermiation (2). At late stage VIII before the release of mature spermatids, p-FAK-Tyr^{407} diminished considerably to a virtually undetectable level at the Sertoli cell-spermatid interface (Fig. 1E). Furthermore, p-FAK-Tyr^{407} was also detected in vesicle-like structures near the tubule lumen in all stages, except stage VIII (Fig. 1 D and E and Fig. S1), which appear to represent secretory or storage vesicles from Sertoli or germ cells. They are possibly cytoplasmic droplets derived from residual p-FAK-Tyr^{407}-containing materials engulfed by Sertoli cells for transcytosis, recycling, or degradation.

Similar to an earlier study using National Institutes of Health (NIH) 3T3 cells (14), phosphorylation of FAK-Tyr^{407} was found to be inversely related to that of FAK-Tyr^{397} in the testis. For instance, in Sertoli cells cultured for increasing periods of time to allow the establishment of TJ and basal ES to create the functional TJ barrier that mimics the BTB in vivo (15, 16), both total FAK and p-FAK-Tyr^{407} were most highly expressed in freshly isolated cells and showed decreasing protein levels

throughout the culture period, whereas p-FAK-Tyr^{397} showed an increasing trend from its lowest level in freshly isolated cells (Fig. 2 A and B). Furthermore, p-FAK-Tyr^{407} and p-FAK-Tyr^{397} show differential localization patterns in the testis, displaying mutually exclusive signals (Fig. 2 C and D). In stage VII to early stage VIII tubules, p-FAK-Tyr^{407} was stained robustly at the BTB and the concave side of elongated spermatid heads, with relatively weak signals at the convex side, whereas p-FAK-Tyr^{397} was mainly detected at the convex side of elongated spermatid heads but not at the BTB at these stages, consistent with results of two earlier studies (3, 4). Thus, p-FAK-Tyr^{407} displays a partial colocalization with Arp3 at the apical TBC (Fig. 2C), suggesting its possible role during Arp2/3-mediated actin nucleation to facilitate protein endocytosis to prepare for spermiation. Conversely, the localization of p-FAK-Tyr^{397} is instead closely matched with β1-integrin at the convex side of spermatid heads at the apical ES (Fig. 2E), consistent with the general phenomenon of FAK autophosphorylation at Tyr^{397} induced by integrin engagement (7, 9). These results suggest that FAK phosphorylated at Tyr^{407} is functionally distinct from its autophosphorylated form at Tyr^{397} in the epithelium during the seminiferous epithelial cycle.

Overexpression of FAK Mutants on Tyr^{407} Alters Phosphorylation Status on Tyr^{397}. Having established that the BTB is a major site where FAK-Tyr^{407} but not -Tyr^{397} is phosphorylated, a series of experiments was conducted to examine the function of Tyr^{407} phosphorylation in BTB dynamics. As a model system, primary Sertoli cells were cultured in vitro under conditions that allow the assembly of a functional TJ barrier with ultrastructures (e.g., TJ, basal ES, gap junction, desmosome) mimicking the BTB in vivo (15, 16); this system is widely used in the field (1, 16). Nonphosphorylatable and phosphomimetic mutants at Tyr^{407} and/or Tyr^{397} were constructed by site-directed mutagenesis in which the Tyr residue was replaced by Phe (Y407F; Y397F) and Glu (Y407E; Y397E), respectively (Fig. S2). These mutants were overexpressed in Sertoli cells, with the empty vector (pCI-neo)

Fig. 1. Expression of phosphorylated FAK and the stage-specific expression pattern of p-FAK-Tyr^{407} in adult rat testes. (A) Immunoblots show the expression of FAK and its phosphorylated forms in adult rat testes, Sertoli cells (SC; isolated from 20-d-old rat testes and cultured for 5 d), and germ cells (GC; freshly isolated from adult rat testes and used within ~2 h). Actin served as a protein loading control. (B) Histogram summarizes immunoblotting results as in A from several independent experiments. Each data point was normalized against the corresponding actin level, and the protein level in the testis was arbitrarily set as 1, against which statistical comparison was performed. Each bar represents a mean ± SD of $n = 3$–4. *$P < 0.05$; **$P < 0.01$ vs. testis; 1-way ANOVA followed by Dunnett's test. (C) Immunoblot shows the specificity of the anti–p-FAK-Tyr^{407} antibody (Table S1). (D) Immunofluorescence staining of p-FAK-Tyr^{407} in frozen sections of adult rat testes (red) is shown. (E) Merged images with nuclei stained with DAPI (blue) are shown. Each image shows a cross-section of the seminiferous epithelium from a tubule with its stage annotated with roman numerals I through XIV. (Insets) Boxed areas in selected images in E were magnified. p-FAK-Tyr^{407} was localized in the basal compartment near the basement membrane, consistent with its localization at the BTB (open arrowheads in D) at all stages. It was also highly expressed, most predominantly at the concave side of elongated spermatid heads in stage VII to early stage VIII tubules (Insets in E), corresponding to structures known as apical TBC at the Sertoli cell-elongating spermatid interface, which is the "degenerating" apical ES (2), but the signal diminished rapidly to a nondetectable level in late stage VIII. In addition, p-FAK-Tyr^{407} appeared in vesicle-like structures near the tubule lumen except at stage VIII, apparently as part of the cytoplasmic droplets that were shredded during spermiogenesis, perhaps representing "degraded" p-FAK-Tyr^{407}. (Scale bar: D and E, 40 μm.)
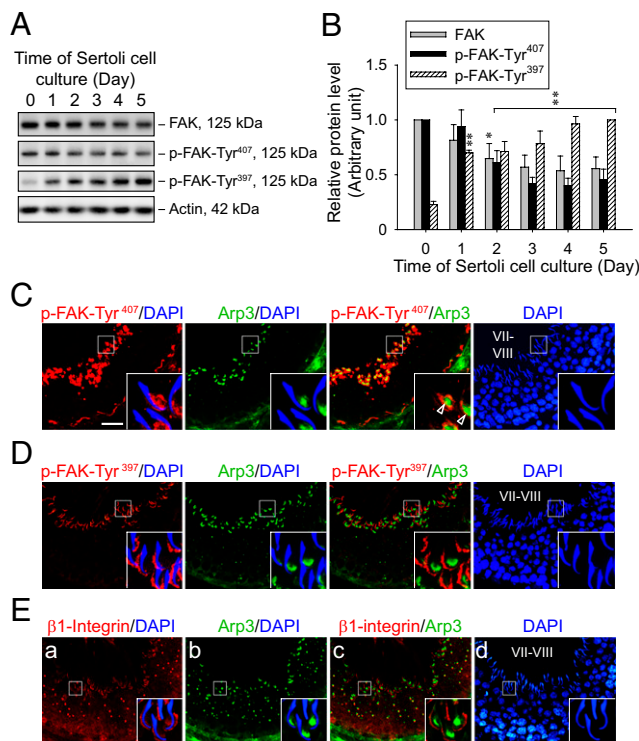
CELL BIOLOGY
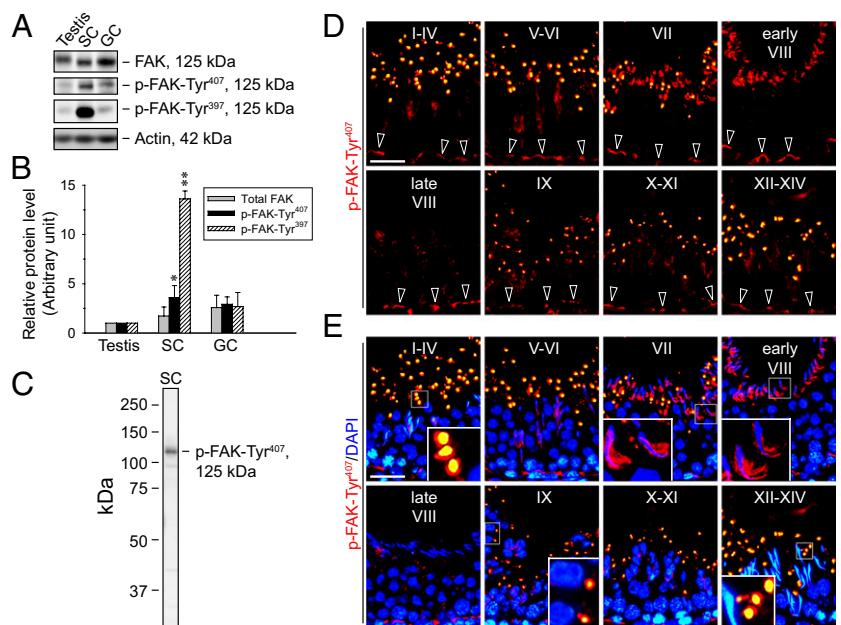
Fig. 2. FAK phosphorylated at Tyr^{407} and Tyr^{397} shows restricted but differential temporal and spatial expression in the seminiferous epithelium of adult rat testes. (*A*) Immunoblots show the change in protein levels of FAK and its phosphorylated forms in Sertoli cells (0.4 × 10^6 cells/cm^2) cultured for specified durations after their isolation. Lysate containing 25 μg of proteins was loaded in each lane. Actin served as a control for subsequent quantification analysis. (*B*) Histogram summarizes immunoblotting results as in *A* from several independent experiments. Each data point was normalized against the corresponding actin level, and the protein level was arbitrarily set at 1 either on day 0 for FAK and p-FAK-Tyr^{407} or on day 5 for p-FAK-Tyr^{397}. Each bar represents a mean ± SD of *n* = 3–4. *$P < 0.05$; **$P < 0.01$ vs. day 0; one-way ANOVA followed by Dunnett's test. Dual-labeled immunofluorescence staining of p-FAK-Tyr^{407} (*C*; red), p-FAK-Tyr^{397} (*D*; red), or β1-integrin (*E*; red) with Arp3 (*C–E*; green) in frozen sections of adult rat testes. Nuclei were visualized with DAPI (blue). (*Insets*) Boxed area in each image in *C–E* was magnified. In stage VII–VIII tubules, both p-FAK-Tyr^{407} and Arp3 were predominantly localized at the concave side of elongated spermatid heads, partially colocalizing with each other (open arrowheads in *C*), whereas p-FAK-Tyr^{397} and β1-integrin were mainly found at the convex side instead. (Scale bar: *C–E*, 40 μm.)

and WT FAK serving as controls. Attempts were made to knock down endogenous FAK concurrent to mutant expression using siRNA duplexes or a micro-RNA expression cassette that effectively targets the 3′UTR of endogenous rat FAK, which is absent in FAK constructs. However, the efficacy of the combined transfections was unacceptably low possibly because of the inherent limitations of primary cultures. Thus, overexpression of FAK constructs was performed alone in this study, resulting in an increase of ∼40% in FAK protein level vs. empty vector (Fig. 3 *A* and *B*). As expected, expression of FAK Y407F (nonphosphorylatable mutant) resulted in a decrease in the p-FAK-Tyr^{407} level vs. the WT construct (Fig. 3 *A* and *C*). It is noted that phosphomimetic mutant FAK Y407E expression did not lead to a further increase in the p-FAK-Tyr^{407} level. This is not surprising, because the antibody should not recognize the epitope that does not contain a phosphate group (Fig. S2). Consistent with the observation here and from an earlier report (14) that the phosphorylation of Tyr^{407} and Tyr^{397} is inversely related, expression of nonphosphorylatable mutant FAK Y407F led to an increase in the p-FAK-Tyr^{397} level, whereas the opposite was

true for the expression of phosphomimetic mutant FAK Y407E (Fig. 3 *A* and *D*). These results suggest that the phosphorylation status of FAK-Tyr^{397} is negatively regulated by Tyr^{407} phosphorylation, which may play a role in attenuating stimulations from integrins or growth factor receptors. Additionally, expression of WT FAK and FAK-Tyr^{407} mutants resulted in a slight increase in the TJ protein occludin (Fig. 3 *A* and *E*). Apart from these, no significant change was detected in the levels of other examined BTB structural proteins and actin-regulating proteins. We also investigated the effects of FAK Y397 mutants on FAK-Tyr^{407} phosphorylation (Fig. S3). As expected, expression of nonphosphorylatable mutant FAK Y397F suppressed p-FAK-Tyr^{397} level vs. the WT construct, whereas the phosphomimetic mutant Y307E did not lead to a further increase in p-FAK-Tyr^{397} (Fig. S3) because the anti–p-FAK-Tyr^{397} antibody should not recognize the epitope that does not contain an actual phosphate group (Fig. S2). Expression of these FAK Y397 mutants was found not to affect the level of p-FAK-Tyr^{407} significantly (Fig. S3). Thus, FAK-Tyr^{397} may not reciprocally regulate the phosphorylation status of FAK-Tyr^{407}.

FAK Mutants on Tyr^{407} and Tyr^{397} Exhibit Antagonistic Effects on Sertoli Cell TJ Barrier Function. The effects of FAK-Tyr^{407} and FAK-Tyr^{397} phosphorylation on the Sertoli cell TJ barrier were investigated by quantifying changes in TJ function across the Sertoli cell epithelium following FAK mutant expression (Fig. 4). Overexpression of WT FAK, per se, perturbed TJ integrity vs. the empty vector (Fig. 4*A*), whereas an earlier report showed that FAK knockdown also disrupted TJ integrity (6), indicating that an optimal level of FAK is necessary for maintaining an intact BTB. Next, we showed that FAK Y407E phosphomimetic mutation and FAK Y397F nonphosphorylatable mutation (i.e., reducing the endogenous p-FAK-Tyr^{397} level in these cells) each promoted TJ integrity vs. the WT, whereas the opposite was true for FAK Y407F mutation (Fig. 4 *B* and *C*). Collectively, these findings illustrate that phosphorylation of FAK-Tyr^{407} and FAK-Tyr^{397} exhibits antagonistic effects in BTB dynamics, with the former being favorable for and the latter being disruptive to TJ integrity. This agrees with the observation that p-FAK-Tyr^{407} but not p-FAK-Tyr^{397} is concentrated at the BTB in vivo (Figs. 1*D* and 2 *C* and *D*). More important, expression of the double-mutant FAK Y397E-Y407E abolished the increase in transepithelial electrical resistance expected from Y407E mutation (Fig. 4*D*), suggesting that the TJ-promoting effect of Tyr^{407} phosphorylation is dependent, at least in part, on the downregulation of Tyr^{397} phosphorylation.

Apart from assessing the TJ barrier function, staining data also supported the notion that Tyr^{407} phosphorylation is important for TJ integrity (Fig. 5 and Figs. S4 and S5). The expression of nonphosphorylatable mutant FAK Y407F resulted in considerably reduced actin filament bundles in transfected Sertoli cells, impeding junction integrity; in contrast, phosphomimetic mutant FAK Y407E increased the intensity of cortical actin filaments beneath the cell surface, possibly reinforcing junction complexes at the cell-cell interface (Fig. 5, *i–iv*). This increase in cortical F-actin might be supported by Arp2/3 complex-mediated actin nucleation, because Arp3 was also induced considerably at the cell-cell interface in FAK Y407E mutant (Fig. 5, *v–viii* and Fig. S5), but the actin capping/bundling protein Eps8 did not show any significant change in localization (Fig. 5, *ix–xii*). These changes in F-actin staining represent the remodeling of actin filaments instead of changes in total actin protein level, because the actin level remained apparently constant when lysates containing an equal amount of protein were loaded for immunoblots (Fig. 3). Finally, FAK Y407F mutation led to the internalization of the TJ proteins claudin-11 (Fig. 5, *xiii–xvi* and Fig. S5) and ZO-1 (Fig. 5, *xvii–xx*), with these adhesion proteins moving away from the cell-cell interface and into the cell cytosol, thereby contributing to a disrupted TJ barrier. In short, these findings are
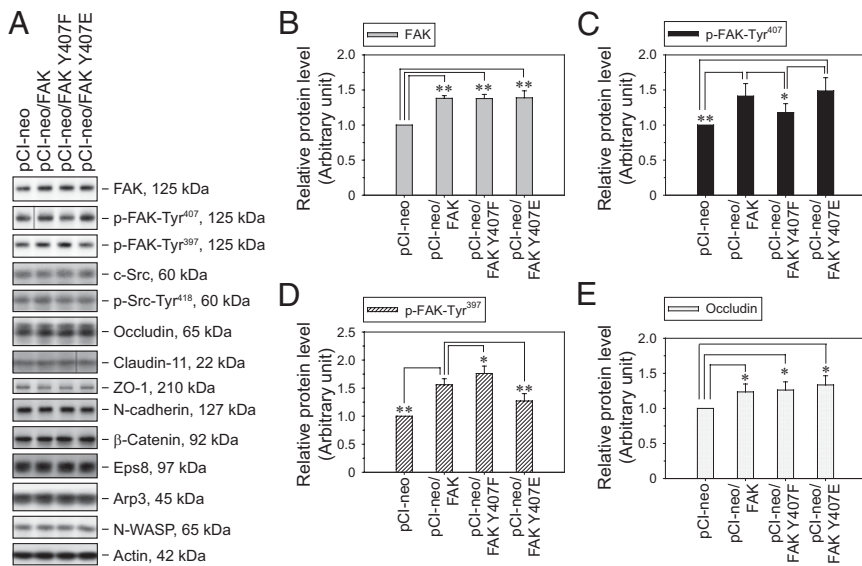
Fig. 3. Effects of FAK-Tyr[407] mutations on the steady-state levels of BTB regulatory and constituent proteins in Sertoli cells in vitro with a functional TJ–permeability barrier. (A) Immunoblot analysis of selected BTB regulatory (e.g., FAK, c-Src, Eps8, Arp3, N-WASP) and constituent (e.g., occludin, claudin-11, ZO-1, N-cadherin, β-catenin) proteins in Sertoli cells following the transfection of pCI-neo vector only and various FAK constructs. Sertoli cells (0.4 × 10⁶ cells/cm²) cultured for 2 d with an established functional TJ–permeability barrier were transfected with plasmid DNA, and lysates harvested 3 d thereafter were subjected to immunoblotting. Actin served as a protein loading control. (B–E) Histograms summarize immunoblotting results as in A from several independent experiments. Proteins that did not show any significant change were not represented in the histograms. Each data point was normalized against the corresponding actin level and then against the protein level in pCI-neo, which was arbitrarily set as 1. Each bar is a mean ± SD of n = 4–6. *P < 0.05; **P < 0.01 vs. pCI-neo (B and E) or pCI-neo/FAK (C and D); one-way ANOVA followed by the Newman–Keuls test.

consistent with the lower magnified images and confocal micrographs shown in Figs. S4 and S5, respectively.

FAK Associates with N-WASP and Regulates Arp2/3-Mediated Actin Nucleation via Tyr[407] Phosphorylation. In a study by coimmunoprecipitation using lysates of seminiferous tubules isolated from adult rat testes, FAK was shown to associate structurally with N-WASP but not with Arp3 and Eps8 (Fig. 6A). Furthermore, N-WASP coimmunoprecipitates with p-FAK-Tyr[407] but not with p-FAK-Tyr[397] (Fig. 6A). These results are in agreement with the differential localization between p-FAK-Tyr[407] and p-

FAK-Tyr[397], with the former colocalizing with Arp3 (Fig. 2). It is noted that the association between FAK and N-WASP was also observed in NIH 3T3 cells (12). Given the coexistence of FAK and N-WASP within the same macromolecular complex in the seminiferous epithelium, the possible influence of FAK on N-WASP–mediated activation of the Arp2/3 complex was next examined. The overexpression of both WT FAK and FAK Y407E phosphomimetic mutant in Sertoli cells induced the association between N-WASP and Arp3, which was below detectable level in cells transfected with empty vector or FAK Y407F nonphosphorylatable mutant (Fig. 6B). Furthermore, N-WASP/Arp3 association increased by approximately threefold following FAK Y407E mutation vs. the WT (Fig. 6C). These results thus suggest that FAK-Tyr[407] phosphorylation might promote Arp2/3 activation by N-WASP, which was further confirmed by an in vitro actin polymerization assay. The effect of cell lysates transfected with FAK constructs on the kinetics of pyrene-actin polymerization was followed by an increase in fluorescence emission at 395–440 nm (Fig. 6D). On the induction of polymerization by the addition of actin polymerization buffer, fluorescence intensity initially increased in a linear manner for a duration ranging between 3 and 5 min (which varied with the ambient temperature and different batches of pyrene-actin) and gradually reached a plateau phase. The initial rate of polymerization in the linear phase of each reaction was then estimated by linear regression. Combined results from several independent experiments showed that FAK Y407F nonphosphorylatable mutation led to a decrease of ~25% in actin polymerization rate vs. the WT (Fig. 6E). However, FAK Y407E mutation did not lead to any further increase in actin polymerization rate as expected, suggesting that certain required factors might be lacking in this in vitro system. Collectively, our results support the notion that FAK-Tyr[407] phosphorylation enhances Arp2/3 activation by N-WASP, increasing actin nucleation and polymerization at the cell-cell interface, thereby promoting Sertoli cell TJ function.
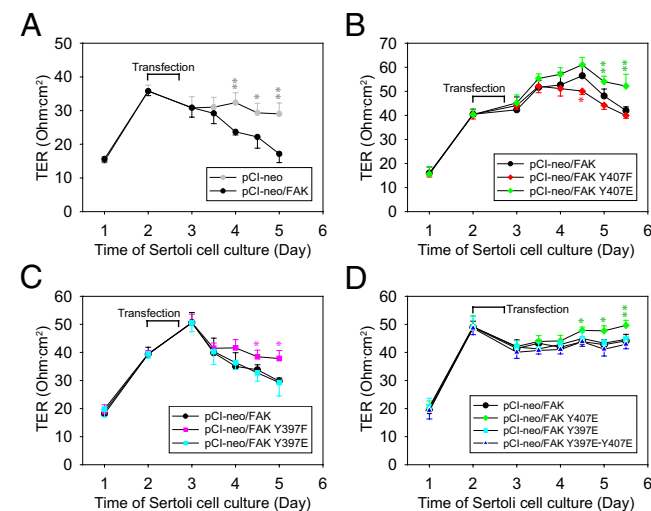
Discussion

This study provides unique details regarding how signaling to the actin cytoskeleton at the BTB can be efficiently modulated by phosphorylation events of FAK at Tyr[407] and Tyr[397]. FAK-Tyr[407] phosphorylation likely serves as a "molecular switch" to activate actin nucleation via the Arp2/3 complex, thereby promoting cortical actin assembly to support cell-cell junction integrity across an epithelium, in part, by suppressing Tyr[397] phosphor-

Fig. 4. Effects of FAK-Tyr[407] and FAK-Tyr[397] mutations on the integrity of the TJ–permeability barrier in Sertoli cells in vitro. Sertoli cells (1.0 × 10⁶ cells/cm²) cultured for 2 d with a functional TJ–permeability barrier were transfected with pCI-neo vector only and various FAK constructs including vector vs. WT (A), WT vs. Y407 mutants (B), WT vs. Y397 mutants (C), and WT vs. Y407, Y397, and double mutants (D). Transepithelial electrical resistance (TER) across the Sertoli cell epithelium was monitored once or twice daily throughout the entire period of culture, and fresh media were replaced thereafter. Data points represent mean ± SD (n = 3–4 replicates in a representative experiment). Similar results were obtained from at least three independent experiments. *P < 0.05; **P < 0.01 vs. pCI-neo/FAK; one-way ANOVA followed by the Newman–Keuls test.
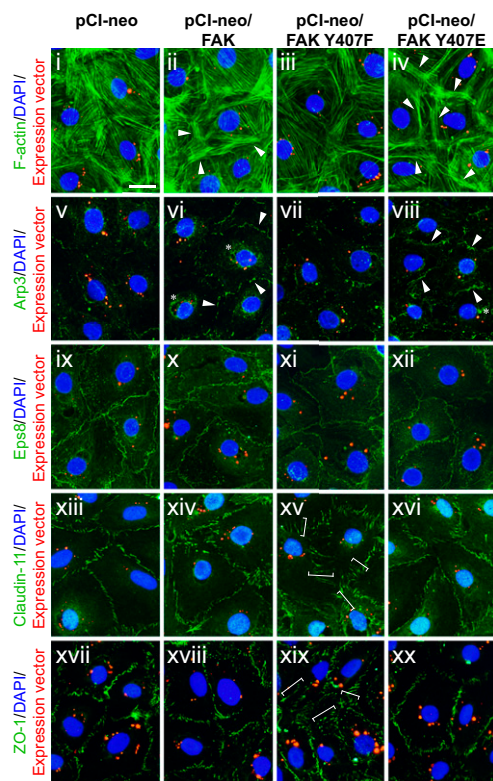
Fig. 5. Effects of FAK-Tyr^{407} mutations on the actin cytoskeleton and the localization of BTB constituent proteins in Sertoli cells in vitro. Sertoli cells (0.04×10^6 cells/cm^2) cultured for 2 d were transfected with Cy3-labeled plasmid DNA of pCI-neo vector only vs. various FAK constructs (red). Two days thereafter, cells were fixed and processed for F-actin staining (*i–iv*; green) or immunofluorescence staining of Arp3 (*v–viii*; green), Eps8 (*ix–xii*; green), claudin-11 (*xiii–xvi*; green), or ZO-1 (*xvii–xx*; green). Nuclei were visualized with DAPI (blue). Overexpression of both WT FAK and FAK Y407E caused up-regulation of cortical actin and Arp3 at the cell-cell interface (arrowheads in *ii*, *iv*, *vi*, and *viii*) and the appearance of Arp3-rich "precipitates" in the cell interior (annotated by asterisks in *vi* and *viii*), whereas overexpression of FAK Y407F caused mislocalization of TJ proteins claudin-11 and ZO-1, moving away from the cell-cell interface into the Sertoli cell cytosol (white brackets in *xv* and *xix*), showing signs of protein internalization. (Scale bar: 30 μm.)

ylation. In a nutshell, it is believed that integrins or growth factors (e.g., TGF-β3) stimulate autophosphorylation of FAK-Tyr^{397}, facilitating the formation of an FAK/Src complex whose intrinsic kinase activity and scaffolding/adaptor function are important for various signal transduction events during cell adhesion and migration (17). However, accumulating evidence suggests that a much more elaborate mechanism is required to fine-tune the activity of FAK because it is involved in multiple steps of the cell motility cycle (18), including adhesion assembly, actin remodeling, and adhesion turnover, which is why simple loss/gain-of-function studies often lead to seemingly contradictory results in the literature. For instance, an increase in FAK activity has been reported to reduce motility, stabilize adhesion, and promote stress fiber assembly (19), possibly via RhoA activation (20); however, on the other hand, FAK deficiency in a number of cell types also led to reduced motility, with impaired adhesion turnover and hyperactivated Rho-Rho associated coiled-coil containing protein kinase (Rho-ROCK) signaling (21, 22). To ensure timely activation of a suitable downstream signaling pathway, it is likely that an efficient mechanism is in place to regulate this multifunctional molecule.

One such regulatory mechanism could be through the phosphorylation of different Tyr and/or Ser residues on FAK (1).

Although FAK-Tyr^{397} and FAK-Tyr$^{576/577}$ phosphorylation are well established as being positively correlated with its intrinsic kinase activity (7), the functions of other phosphorylation sites are less understood. Of the several FAK phosphorylation forms we attempted to characterize (which also included p-FAK-Ser^{722} and p-FAK-Ser^{910} in pilot experiments), p-FAK-Tyr^{407} displayed a localization pattern in the seminiferous epithelium during the epithelial cycle considerably different from both total FAK and p-FAK-Tyr^{397}, prompting our interest to pursue its function. Herein, we show that FAK-Tyr^{407} phosphorylation strengthens the TJ barrier at the Sertoli-Sertoli cell interface, possibly by reinforcing the underlying actin cytoskeleton, whereas Tyr^{397} facilitates the disruption of the TJ barrier function. These results are in line with several earlier reports. First, it was shown that FAK-Tyr^{407} phosphorylation suppresses Tyr^{397} phosphorylation to negatively regulate its enzymatic and biological activities during cellular events, such as contact inhibition and cell cycle arrest (14). Furthermore, FAK-Tyr^{397} phosphorylation was found to be associated with virus-induced TJ barrier disruption at the blood–brain barrier (23), as well as with Src-induced AJ disruption in colon cancer cells (24). These findings are analogous to our data illustrating that selective phosphorylation of FAK-Tyr^{407} but not Tyr^{397} at the BTB promotes cell junction integrity, stabilizing the Sertoli cell epithelium rather than promoting migration and restructuring. It is likely that the interplay between FAK-Tyr^{407} and FAK-Tyr^{397} in regulating Sertoli cell TJ barrier function at the BTB may involve other yet to be identified regulatory partners, such as c-Src and c-Yes. Thus, further investigation is warranted to identify additional phosphorylation events and the signaling input(s) from other protein kinases that are involved.

In this study, we mainly focused on the effects of FAK phosphorylation in BTB dynamics using the Sertoli cell culture system. In the seminiferous epithelium in vivo, p-FAK-Tyr^{407} and p-FAK-Tyr^{397} found at the Sertoli cell-spermatid interface, namely, the apical ES, also seem to have functions distinct from each other. At the concave side of elongated spermatid heads, p-FAK-Tyr^{407} is apparently needed for the activation of the Arp2/3 complex, giving rise to the actin network surrounding the tubular invaginations, known as apical TBCs (2, 25), assisting the degeneration of the "old" apical ES to facilitate endocytosis of adhesion proteins at the site, and their subsequent transcytosis and recycling (2, 25), so that these proteins can be reused to form "new" apical ES, resulting from "newly" differentiated step 8 spermatids at spermiogenesis. Conversely, p-FAK-Tyr^{397} is restricted to the convex side of elongated spermatid heads (3, 4). This likely represents FAK autophosphorylation that results from α6β1-integrin clustering on the Sertoli cell plasma membrane by its ligand laminin-333 on the germ cell surface (26). The function of p-FAK-Tyr^{397} at this site is not well understood, but it may be associated with the release of mature spermatids from the epithelium at spermiation (1, 5). Based on results in this study, we provide unique details in the apical ES-BTB functional axis in the seminiferous epithelium (27) regarding how spermatid release and BTB restructuring, which occur simultaneously at the opposite ends of the epithelium, are coordinated during stage VIII of the rat seminiferous epithelial cycle (1). On the release of spermatids, the dissolution of the protein complex consisting of integrin/laminin/p-FAK-Tyr^{397} may lead to a transient surge of free p-FAK-Tyr^{397} in the Sertoli cell cytoplasm, which induces restructuring of BTB junction complexes to allow the entry of preleptotene spermatocytes into the adluminal compartment. The restoration of a stable BTB may be mediated by the attenuation of FAK-Tyr^{397} phosphorylation by p-FAK-Tyr^{407} at the BTB and/or other feedback regulation. This possibility should be carefully evaluated in future studies.

In summary, this report demonstrates the involvement of p-FAK-Tyr^{407} and p-FAK-Tyr^{397} in regulating BTB dynamics in the rat testis, having antagonistic effects on BTB restructuring during the seminiferous epithelial cycle. These findings also

Fig. 6. Association of FAK with the actin nucleation machinery in the testis and the effects of FAK-Tyr[407] mutations on actin polymerization at the Sertoli cell BTB. (*A*) Seminiferous tubules (ST) isolated from adult rat testes were subjected to coimmunoprecipitation with specified antibodies (lanes 2–6) (Table S1), with normal mouse (Ms) or rabbit (Rb) IgG serving as a negative control. Lane 1, positive control containing 50 μg of protein of ST lysate without coimmunoprecipitation. The presence of FAK, p-FAK-Tyr[407], and p-FAK-Tyr[397] in the immunoprecipitate protein complexes was detected by immunoblotting. (*B*) Sertoli cells (0.4×10^6 cells/cm^2) cultured for 2 d with an established TJ–permeability barrier were transfected with pCI-neo vector only vs. various FAK constructs. Lysates harvested 3 d thereafter were subjected to coimmunoprecipitation with an anti–N-WASP antibody (lanes 2–5), with normal Rb IgG serving as the negative control (lane 6). Lane 1, positive control represents 10 μg of protein of Sertoli cell lysate without coimmunoprecipitation. The presence of Arp3 in the precipitate was detected by immunoblotting. Actin served as a protein loading control. (*C*) Histogram summarizes coimmunoprecipitation results as in *B* from several independent experiments. Each data point was normalized against the corresponding actin level, and the N-WASP/Arp3

association level in pCI-neo/FAK was arbitrarily set as 1, against which statistical comparison was performed. Each bar is a mean ± SD of $n = 4$. **$P < 0.01$ vs. pCI-neo/FAK; two-tailed Student t test. (*D*) Sertoli cells (0.4×10^6 cells/cm^2) cultured for 2 d were transfected with pCI-neo vector only vs. various FAK constructs. Lysates harvested 3 d thereafter were subjected to a fluorometric-based actin polymerization assay, in which the polymerization of pyrene-labeled actin was monitored by enhanced fluorescence emission at 395–440 nm. (*E*) Histogram summarizes results as in *D* from several independent experiments. The rate of actin polymerization (increase in fluorescence intensity over time) during the initial linear phase in the first 3–5 min was estimated by linear regression. The rate of actin polymerization in pCI-neo/FAK was arbitrarily set as 1. Each bar is a mean ± SD of $n = 4$ for pCI-neo; $n = 7$ for all other groups. **$P < 0.01$ vs. pCI-neo/FAK; one-way ANOVA followed by the Newman–Keuls test.
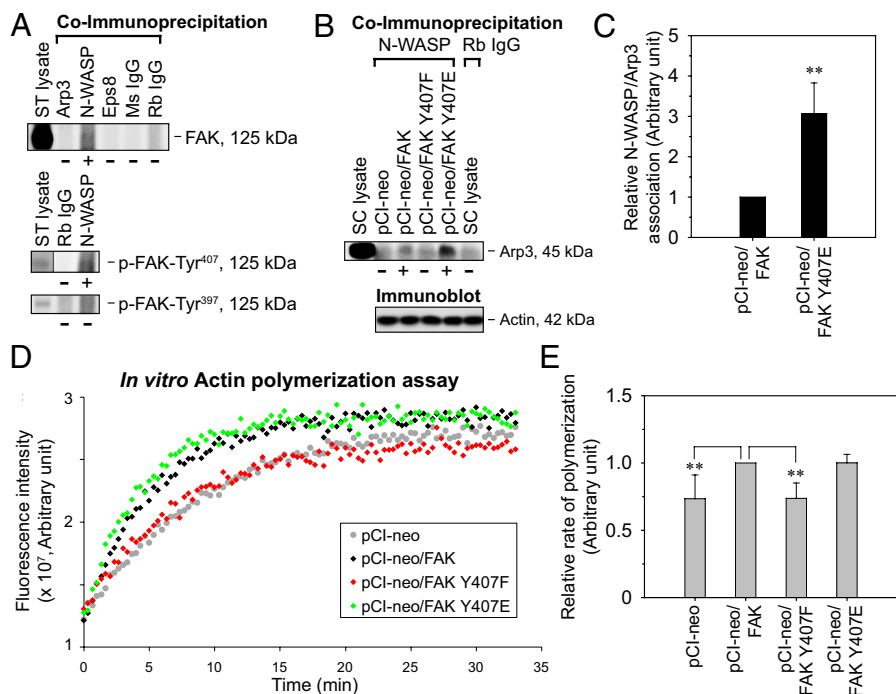
provide the framework on which experiments can be designed to investigate the role of FAK in human BTB function.

Materials and Methods

A discussion of materials (Tables S1 and S2) and methods, such as cell cultures, preparation of cDNA constructs, and transfections, can be found in *SI Materials and Methods*. Detailed data analysis on fluorescence images,

confocal micrographs, actin polymerization assay, and statistics can also be found in *SI Materials and Methods*.

1. Cheng CY, Mruk DD (2012) The blood-testis barrier and its implications for male contraception. *Pharmacol Rev* 64:16–64.
2. Cheng CY, Mruk DD (2010) A local autocrine axis in the testes that regulates spermatogenesis. *Nat Rev Endocrinol* 6:380–395.
3. Siu MKY, Mruk DD, Lee WM, Cheng CY (2003) Adhering junction dynamics in the testis are regulated by an interplay of β 1-integrin and focal adhesion complex-associated proteins. *Endocrinology* 144:2141–2163.
4. Beardsley A, Robertson DM, O'Donnell L (2006) A complex containing α6β1-integrin and phosphorylated focal adhesion kinase between Sertoli cells and elongated spermatids during spermatid release from the seminiferous epithelium. *J Endocrinol* 190:759–770.
5. O'Donnell L, Nicholls PK, O'Bryan MK, McLachlan RI, Stanton PG (2011) Spermiation: The process of sperm release. *Spermatogenesis* 1:14–35.
6. Siu ER, Wong EWP, Mruk DD, Porto CS, Cheng CY (2009) Focal adhesion kinase is a blood-testis barrier regulator. *Proc Natl Acad Sci USA* 106:9298–9303.
7. Mitra SK, Hanson DA, Schlaepfer DD (2005) Focal adhesion kinase: In command and control of cell motility. *Nat Rev Mol Cell Biol* 6:56–68.
8. Tomar A, Schlaepfer DD (2009) Focal adhesion kinase: Switching between GAPs and GEFs in the regulation of cell movement. *Curr Opin Cell Biol* 21:676–683.
9. Schaller MD (2010) Cellular functions of FAK kinases: Insight into molecular mechanisms and novel functions. *J Cell Sci* 123:1007–1013.
10. Quadri SK (2012) Cross talk between focal adhesion kinase and cadherins: Role in regulating endothelial barrier function. *Microvasc Res* 83:3–11.
11. Goley ED, Welch MD (2006) The ARP2/3 complex: An actin nucleator comes of age. *Nat Rev Mol Cell Biol* 7:713–726.
12. Wu X, Suetsugu S, Cooper LA, Takenawa T, Guan JL (2004) Focal adhesion kinase regulation of N-WASP subcellular localization and function. *J Biol Chem* 279:9565–9576.
13. Serrels B, et al. (2007) Focal adhesion kinase controls actin assembly via a FERM-mediated interaction with the Arp2/3 complex. *Nat Cell Biol* 9:1046–1056.
14. Lim Y, et al. (2007) Focal adhesion kinase is negatively regulated by phosphorylation at tyrosine 407. *J Biol Chem* 282:10398–10404.
15. Lie PPY, Cheng CY, Mruk DD (2010) Crosstalk between desmoglein-2/desmocollin-2/Src kinase and coxsackie and adenovirus receptor/ZO-1 protein complexes, regulates blood-testis barrier dynamics. *Int J Biochem Cell Biol* 42:975–986.
16. Mruk DD, Cheng CY (2011) An *in vitro* system to study Sertoli cell blood-testis barrier dynamics. *Methods Mol Biol* 763:237–252.
17. Mitra SK, Schlaepfer DD (2006) Integrin-regulated FAK-Src signaling in normal and cancer cells. *Curr Opin Cell Biol* 18:516–523.
18. Carragher NO, Frame MC (2004) Focal adhesion and actin dynamics: A place where kinases and proteases meet to promote invasion. *Trends Cell Biol* 14:241–249.
19. Siesser PMF, et al. (2008) A FAK/Src chimera with gain-of-function properties promotes formation of large peripheral adhesions associated with dynamic actin assembly. *Cell Motil Cytoskeleton* 65:25–39.
20. Zhai J, et al. (2003) Direct interaction of focal adhesion kinase with p190RhoGEF. *J Biol Chem* 278:24865–24873.
21. Schober M, et al. (2007) Focal adhesion kinase modulates tension signaling to control actin and focal adhesion dynamics. *J Cell Biol* 176:667–680.
22. Webb DJ, et al. (2004) FAK-Src signalling through paxillin, ERK and MLCK regulates adhesion disassembly. *Nat Cell Biol* 6:154–161.
23. Ivey NS, et al. (2009) Association of FAK activation with lentivirus-induced disruption of blood-brain barrier tight junction-associated ZO-1 protein organization. *J Neurovirol* 15:312–323.
24. Avizienyte E, et al. (2002) Src-induced de-regulation of E-cadherin in colon cancer cells requires integrin signalling. *Nat Cell Biol* 4:632–638.
25. Young JS, Guttman JA, Vaid KS, Vogl AW (2009) Tubulobulbar complexes are intercellular podosome-like structures that internalize intact intercellular junctions during epithelial remodeling events in the rat testis. *Biol Reprod* 80:162–174.
26. Yan HHN, Cheng CY (2006) Laminin α 3 forms a complex with β3 and γ3 chains that serves as the ligand for α 6β1-integrin at the apical ectoplasmic specialization in adult rat testes. *J Biol Chem* 281:17286–17303.
27. Yan HHN, Mruk DD, Wong EWP, Lee WM, Cheng CY (2008) An autocrine axis in the testis that coordinates spermiation and blood-testis barrier restructuring during spermatogenesis. *Proc Natl Acad Sci USA* 105:8950–8955.

CELL BIOLOGY